Time-Resolved Mode Space based Quantum-Liouville type Equations applied onto DGFETs

1st Lukas Schulz
High Frequency Institute
TU Dortmund
Dortmund, Germany
lukas.schulz@tu-dortmund.de

2nd Dirk Schulz
High Frequency Institute
TU Dortmund
Dortmund, Germany
dirk2.schulz@tu-dortmund.de

***Abstract*—The investigation of a time-resolved quantum transport analysis is a major issue for the future progress in engineering tailored nanoelectronic devices. In this contribution, the time dependence is addressed along with the single-time formulation of quantum mechanics based on the von-Neumann equation in center-mass coordinates. This equation is investigated utilizing a distinct set of basis functions leading to so-called Quantum-Liouville type equations, which are combined with the mode space approximation to investigate the time-resolved behavior of double gate field effect transistors including the self-consistent Hartree potential.**

***Index Terms*—double gate field effect transistor, mode space expansion, numerical methods, time-resolved quantum transport, von-Neumann equation, Wigner equation**

I. Introduction

Switching processes in today's sophisticated transistors are the heart of modern information technology. Unfortunately, they are responsible for the essential dissipation of power. To account for these effects, quantum kinetic numerical methods are desirable. In principle, the corresponding quantum kinetics can be subdivided into two major approaches, as there are double-time methods, such as the non-equilibrium Green's function (NEGF) formalism [1], as well as single-time methods based on the statistical density matrix, i.e. the Wigner formalism [2]. Time-resolved simulations based on the NEGF formalism are numerically challenging [3]. To overcome these restrictions, methods based on the wavefunction have been introduced [4], [5]. The Wigner formalism provides a quantum description of the system in terms of a phase space formulation [6]. In contrast to the NEGF formalism, the time-resolved quantum transport can be readily determined in both, the coherent as well as the incoherent regime. Indeed, the latter can be addressed along with the simple inclusion of a problem dependent collision operator. However, the adequate choice of the collision operator is a vivid field of discussion [7].

Recently, efforts have been made to numerically solve the von-Neumann equation in center-mass coordinates [8]–[10]. Indeed, this approach seems to be highly versatile, since numerical advantages of a real-space approach can be combined with those of a phase space representation due to simple algebraic basis transformations [8]. Consequently, these different algebraic basis transformations lead to the introduction of the so-called Quantum-Liouville type Equations (QLTE).

Following this approach, the QLTE are combined with the mode space approximation (MSA) [11], [12]. to investigate the time-resolved behavior of a double gate field effect transistor (DGFET). The self-consistent Hartree potential is considered, whereas mode coupling effects and scattering mechanisms are neglected at this stage for a straightforward comparison along with the NEGF formalism within the stationary regime.

II. Theory

In the following, the major relations with regard to the presented approach are briefly discussed.

A. Time-Resolved Mode Space Approximation

When quantum transport is considered in multiple spatial directions, the numerical effort of the solution procedure is in general quiet expensive. As a consequence, accurate methods reducing the overall numerical costs are needed. Right here, the MSA comes into play [11], [12]. Along with the MSA the Hamiltonian with regard to the lateral direction is expanded in terms of basis functions leading to a set of effective one-dimensional equations. When the carriers are confined with regard to the lateral direction, the corresponding lateral eigenvectors are employed to expand the Hamiltonian. These eigenvectors are also known as the modes and, typically, only a few eigenvectors with the lowest energy eigenvalues characterize the transport behavior, which can be estimated from the value of the Fermi-level. Considering the structure

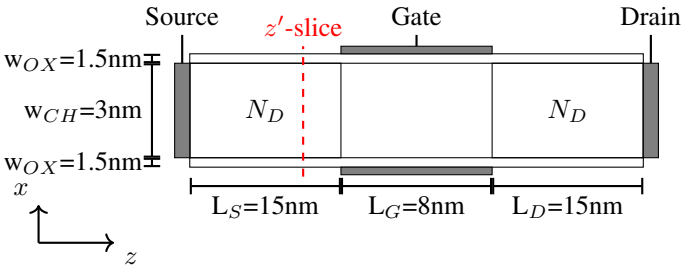

Fig. 1. Schematic diagram of the investigated DGFET including the structural parameters. The dashed line conceptually reflects the slice formalism.

of the analyzed DGFET, as shown in Fig. 1, the corresponding

The authors gratefully acknowledge the financial support by the German Research Funding Association Deutsche Forschungsgemeinschaft under grant SCHU-2016/8-1.

Schrödinger equation within the effective mass approximation reads

$$\left\{-\mathrm{j}\hbar\frac{\partial}{\partial t}-\frac{\hbar^2}{2m_z^\nu}\frac{\partial^2}{\partial z^2}\underbrace{-\frac{\hbar^2}{2m_x^\nu}\frac{\partial^2}{\partial x^2}+V(x,z,t)}_{\mathcal{H}_C}\right\}\Psi^\nu(x,z,t)=0, \tag{1}$$

where x is the confinement direction and z represents the transport direction. The effective masses m_x^ν and m_z^ν depend on the ν-th valley. The potential V includes the conduction band potential, the effect from transient external fields as well as the self-consistent Hartree-Fock potential V_H. The Hamiltonian $\mathcal{H}_C$ captures the confinement and can be diagonalized for each slice z, as depicted in Fig. 1, and timestep t, which enter the equation parametrically, according to

$$\mathcal{H}_C\Phi_m^\nu(x;z,t)=E_m^\nu(z,t)\Phi_m^\nu(x;z,t)=E_m^\nu(z,t)\,|m,\nu\rangle \tag{2}$$

with $E_m^\nu(z,t)$ being the eigenenergy and $|m,\nu\rangle$ representing the spatial distribution of the m-th mode. Distinct modes are orthonormal $\langle\nu,n|\nu,m\rangle=\delta_{n,m}$. Introducing the expansion coefficient $\varphi_m^\nu(z,t)$, the wavefunction can be expanded as

$$\Psi^\nu(x,z,t)=\sum_m\varphi_m^\nu(z,t)\,|m,\nu\rangle\,, \tag{3}$$

and inserted in (1). Exploiting the orthogonality condition as well as (2), an equation of motion for the expansion coefficient $\varphi_m^\nu(z,t)$ can be derived

$$\mathrm{j}\hbar\frac{\partial}{\partial t}\varphi_m^\nu=\left\{-\frac{\hbar^2}{2m_z^\nu}\frac{\partial^2}{\partial z^2}+E_m^\nu(z,t)\right\}\varphi_m^\nu(z,t)=\mathcal{H}_m^\nu\varphi_m^\nu, \tag{4}$$

where due to the parametric dependence the relations $\frac{\partial}{\partial t}|m,v\rangle=0$ and $\frac{\partial}{\partial z}|m,v\rangle=0$ are assumed leading to the uncoupled MSA. The limitations of the latter spatial approximation are discussed elsewhere [11].

B. Quantum-Liouville type Equations

To solve the transport governed by (4), the equation of motion for the statistical density matrix is employed [13]

$$\mathrm{j}\hbar\frac{\partial}{\partial t}\rho=[\mathcal{H},\rho]+\mathrm{j}\hbar\Gamma\left(\rho\right), \tag{5}$$

where the operator Γ contains all interaction mechanisms, such as for instance electron-phonon scattering. Here, only the open system related to in and out scattering at the device boundaries is considered.

Introducing the center-mass coordinates $z=\chi+\frac{1}{2}\xi$ and $z'=\chi-\frac{1}{2}\xi$ as part of the Weyl transform, the von-Neumann equation can be rewritten accordingly as

$$\frac{\partial}{\partial t}\rho_m^\nu(\chi,\xi,t)=\frac{\mathrm{j}\hbar}{m_z^\nu}\frac{\partial^2}{\partial\chi\partial\xi}\rho_m^\nu+\frac{1}{\mathrm{j}\hbar}\left\{E_m^\nu\left(\chi+\frac{1}{2}\xi,t\right)-E_m^\nu\left(\chi-\frac{1}{2}\xi,t\right)-\mathrm{j}W(\xi)\right\}\rho_m^\nu, \tag{6}$$

where the complex absorbing potential [9] is introduced to account for appropriate boundary conditions in the ξ-space. Here, the statistical density matrix is defined as $\rho_m^\nu(\chi,\xi,t)=\varphi_m^\nu(\chi+\frac{1}{2}\xi)\varphi_m^{\nu\dagger}(\chi-\frac{1}{2}\xi)$. From the statistical density matrix, the current density j and the carrier density n can be obtained as

$$n_m^\nu(\chi,t)=\rho_m^\nu\Big|_{\xi=0}\quad\text{and}\quad j_m^\nu(\chi,t)=\frac{\hbar}{m_z^\nu}\Im\left\{\frac{\partial}{\partial\xi}\rho_m^\nu\Big|_{\xi=0}\right\}. \tag{7}$$

The von-Neumann equation (6) is discretized within the real space applying a finite volume scheme with regard to the ξ-direction [9] leading to a discretized statistical density matrix $\boldsymbol{\rho}_m^\nu(\chi,t)$. With regard to the in- and out-scattering at the device contacts, the concept of the inflow boundary conditions is employed [14]. In this manner, the statistical density matrix must be transformed into a presentation, which allows the distinction with respect to the flow behavior. Introducing the transformation matrix $[\boldsymbol{T}]$

$$\boldsymbol{\rho}_m^\nu(\chi,t)=[\boldsymbol{T}]\cdot\boldsymbol{a}_m^\nu(\chi,t), \tag{8}$$

the vector of expansion coefficients $\boldsymbol{a}_m^\nu(\chi,t)$ can be assigned to the flow behavior. For the numerical discretization of the remaining transformed coupled transport equations, the introduction of the phase space exponential operator [9] leads to the formulation

$$\frac{\mathrm{d}}{\mathrm{d}t}\boldsymbol{A}_m^\nu(t)=[\boldsymbol{\Gamma}_m^\nu(t)]\cdot\boldsymbol{A}_m^\nu(t)+\boldsymbol{B}_m^\nu, \tag{9}$$

where the supervector $\boldsymbol{A}_m^\nu(t)$ contains the vectors for all expansion coefficients $\boldsymbol{a}_m^\nu(\chi,t)$ for each slice of the discretized χ-direction. The supervector $\boldsymbol{B}$ represents the inflow boundary conditions. The system (9) can be readily solved in the stationary case ($\frac{\mathrm{d}}{\mathrm{d}t}\boldsymbol{A}=0$) as well as the transient case applying standard approaches, i.e. Crank-Nicolson schemes [15] or Low-Storage-Runge-Kutta methods [9].

C. Inclusion of Self-consistency

Assuming an instantaneous adaption of the field to the carrier-density it is sufficient to solve the Poisson equation for the Hartree potential instead of a wave equation in both, the transient and in the stationary case [16]

$$\nabla\cdot(\epsilon(x,z)\nabla V_H)=q^2\left(n(x,z,t)-N_D(x,z)\right). \tag{10}$$

The total carrier density $n(x,z,t)$ is calculated from the corresponding modal carrier density in each valley by

$$n(x,z,t)=\sum_{\nu,m}n_m^\nu(z,t)\cdot|\Phi_m^\nu(x;z,t)|^2\,, \tag{11}$$

where $n_m^\nu(\chi,t)=n_m^\nu(z,t)$ is utilized. The function $N_D(x,z)$ represents the spatial doping profile. The current density is obtained by accumulating the modal current-densities in each valley. As usual, the Newton-Raphson method is employed along with Dirichlet boundary conditions at the gate contact and von-Neumann boundary conditions at all remaining boundaries (Fig. 1) in the stationary regime

$$\begin{aligned}V_H(x,z)\Big|_{x,z\in\text{gate}}&=E_f+q\phi_\text{m}-q\chi_\text{ch}-qU_\text{gate},\\ \frac{\partial V_H(x,z)}{\partial\eta}\Big|_{x,z\notin\text{gate}}&=0\end{aligned} \tag{12}$$

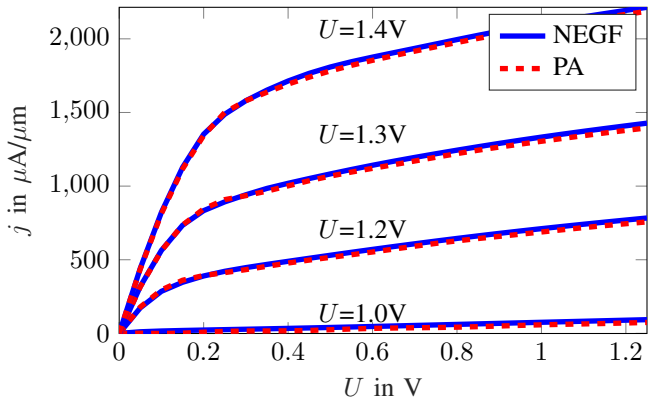

Fig. 2. Comparison of the stationary current densities.

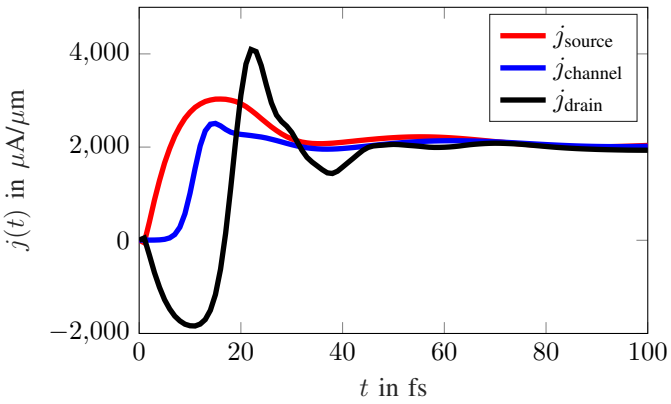

Fig. 3. Current density in dependence of the time within different locations of the bias due to a switch of the gate bias $U_{\text{gate}} = 0.8$V to 1.4V at $t = 0$fs. A constant source-drain bias U =1.0V is applied.

with η being a coordinate belonging to a direction perpendicular to the boundary. The parameters E_f, $q\phi_{\text{m}}$ and $q\chi_{\text{ch}}$ define the Fermi-level, the work function of the metal and the affinity of the channel, respectively. The voltage U_{gate} is applied at the gate contacts. For the evaluation of the expression $\frac{\text{d}}{\text{d}V_H} n$ as part of the Jacobian matrix appearing in the Newton-Raphson method, a Maxwell distribution is presumed for the carrier density [16], so that the relation $\frac{\text{d}}{\text{d}V_H} n = \frac{n}{k_B T}$ holds.

For the transient solution, the Newton-Raphson method cannot be utilized as discussed in [16]. As a consequence, a direct solution procedure is employed, where the Poisson equation is solved once for each time step applying Dirichlet boundary conditions at the drain and source contacts utilizing the relations

$$\begin{aligned} V_H(x,z,t)\Big|_{x,z\in\text{gate}} &= E_f + q\phi_{\text{m}} - q\chi_{\text{ch}} - qU_{\text{gate}}(t) \\ V_H(x,z,t)\Big|_{x,z\in\text{source/drain}} &= -qU_{\text{source/drain}}(t), \\ \frac{\partial V_H(x,z,t)}{\partial \eta}\Big|_{x,z\notin\text{gate,source,drain}} &= 0 \end{aligned} \tag{13}$$

since the use of von-Neumann boundary conditions at the contacts implies charge neutrality near the contacts, which may not hold for the time-resolved behavior.

III. Stationary Regime: Comparison to the NEGF approach

For the evaluation of the proposed approach, the DGFET with the structural parameters as defined in Fig. 1 is analyzed. The material of the gate-contact is Ag, for which the work function $q\phi_{\text{m}} = 4.74$eV is given. The insulator material is SiO_2 ($\epsilon = 3.9\epsilon_0$) and the electron affinity of the channel material $Ga_{0.47}In_{0.53}As$ ($\epsilon = 13.9\epsilon_0$) is assumed to be $q\chi_{\text{ch}}$ =4.5eV. A constant doping concentration $N_D = 2 \cdot 10^{25}\text{m}^{-3}$ is assumed within source and drain regions. The ambient temperature is $T = 300K$ and the isotropical effective masses of the oxid and channel are given by $0.5m_0$ and $0.041m_0$, respectively. Up to three modes have been taken into account. From the results obtained for these cases, it can be concluded that the device behavior is dominated by the first mode. Hence, the inclusion of a larger modal basis does not provide significant more information in the considered case and is, therefore, neglected.

To assess the accuracy of our proposed method, a comparison to the results obtained from the NEGF approach [12] is performed in the stationary regime. The discretization widths $\Delta\chi(= \Delta z) = 0.1$nm and $\Delta y = 0.25$nm are employed, whereas the ξ-direction is discretized within the interval $[-60, 60]$nm utilizing $N_\xi = 400$ discretization points. Here, the results are shown for an expansion of the statistical density matrix in terms of a $N = 200$ orthogonal plane wave basis. Further bases have been investigated, such as sinusoidal-like basis functions given by the eigenvectors of the discretized diffusion matrix. Since they do not provide a deeper insight, the results are not shown. However, for the cases considered, a slightly better convergence rate is observed for the plane wave basis.

In Fig. 2, the current densities obtained from the NEGF approach are compared to the current densities obtained from the proposed approach (PA) applying different gate biases U_{gate} as well as different drain-source biases U.

For all considered cases, a fairly good agreement can be observed from Fig. 2. Due to this agreement, the proposed approach can be validated, predestinating this approach for the time-resolved device analysis.

IV. Transient Response of a DGFET

Essentially, two major switching mechanisms can be investigated: the source-drain bias U is constant and the gate voltage U_{gate} is time-dependend and vice versa. The initial statistical density matrix at $t = 0$fs is obtained from the stationary solution of (9) ($\frac{\text{d}}{\text{d}t} = 0$) in the self-consistent case for the corresponding applied bias situation. Then, for $t > 0$fs the device is driven towards non-equilibrium by either switching the gate bias or the source-drain bias. The transport equation (9) is solved mutually along with the Poisson equation for each discrete timestep applying (13).

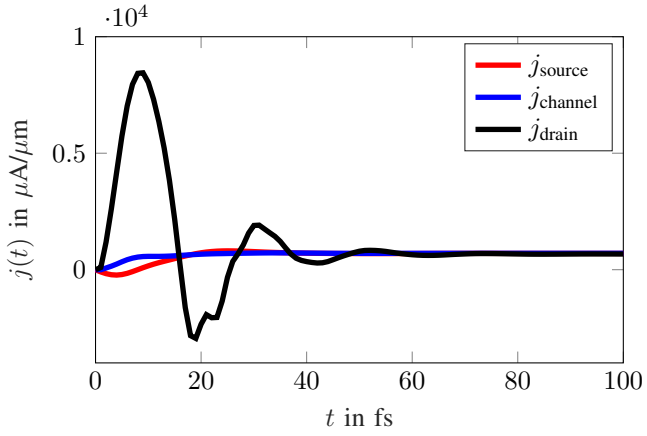

Fig. 4. Transient evolution of the current density within different locations for a constant gate bias $U_{\text{gate}} = 1.2V$ and a switch of the source-drain bias from $U = 0.0$V to $U = 1.0$V.

A. Switching the Gate Voltage

To start with, the "OFF" to "ON"-state switching process is analyzed. Initially, the DGFET is in a steady state at $t = 0$fs applying a constant voltage between source and drain of $U = 1.0$V and a gate bias $U_{\text{gate}} = 0.8$V. At $t > 0$fs the gate voltage is switched to a constant value of $U_{\text{gate}} = 1.4$V. The corresponding time-resolved evolution of the current density at different locations within the DGFET, as there are the source, the middle of the channel and the drain, are depicted in Fig. 3. As it can be seen from the spatially non-constant current densities, the device is in a strong non-equilibrium condition. After approximately 50fs, the major transient effects are decayed and the current densities convergence towards the steady state current density. From Fig. 2 the corresponding stationary current can be determined to a value of approximately 2000μA/μm, which coincides along with the steady state result obtained from the time-resolved approach.

B. Switching the Source-Drain Voltage

Now, the gate bias is kept constant $U_{\text{gate}} = 1.2$V and the voltage between source and drain is switched at $t > 0$fs from 0.0V to 1.0V. As before, the time-resolved evolution of the current density is depicted for the same spatial location in Fig. 4. Remarkably, the transient current density at the drain j_{drain} takes extremely large values in comparison to the steady state current of approximately 700μA/μm, which again coincides with the stationary current as can be observed from Fig. 2. In practice, these large temporal spikes of the current are undesirable since they lead to a large power consumption as well. However, when interaction mechanisms are considered, the current density is effectively reduced. Nonetheless, when phonon-emission processes are considered, the increasing device temperature plays a decisive role.

V. Summary and Conclusion

A self-consistent, time-resolved mode space approach based on Quantum-Liouville type equations has been analyzed, demonstrated and validated. For the stationary regime, an excellent coincidence with the non-equilibrium Green's function approach has been obtained. The approach has been extended to the transient case enabling a deeper insight into the device performance. Since the time-resolved Green's function formalism is computationally extremely demanding, the proposed approach represents a beneficial alternative in this particular case.

References

[1] P. Vogl and T. Kubis, "The non-equilibrium green's function method: An introduction," *J. Comput. Electron*, vol. 9, no. 3-4, pp. 237–242, 2010.

[2] J. Weinbub and D. Ferry, "Recent advances in wigner function approaches," *Appl. Phys. Rev.*, vol. 5, no. 4, p. 041 104, 2018.

[3] E. P. et al., "Time-dependent transport in graphene nanoribbons," *Phys. Rev. B*, vol. 82, p. 035 446, 3 Jul. 2010. DOI: 10.1103/PhysRevB.82.035446.

[4] B. Novakovic and G. Klimeck, "Atomistic quantum transport approach to time-resolved device simulations," in *Proc. of SISPAD*, 2015, pp. 8–11.

[5] B. G. et al., "Numerical simulations of time-resolved quantum electronics," *Physics Reports*, vol. 534, no. 1, pp. 1–37, 2014. DOI: https://doi.org/10.1016/j.physrep.2013.09.001.

[6] E. P. Wigner, "On the quantum correction for thermodynamic equilibrium," in *Part I: Physical Chemistry. Part II: Solid State Physics*, Springer, 1997, pp. 110–120.

[7] R. I. et al., "Wigner-function formalism applied to semiconductor quantum devices: Need for nonlocal scattering models," *Phys. Rev. B*, vol. 96, p. 115 420, 11 Sep. 2017. DOI: 10.1103/PhysRevB.96.115420.

[8] L. Schulz and D. Schulz, "Subdomain algorithm for the numerical solution of the liouville-von-neumann equation," *Proc. of IWCN*, 2019.

[9] ——, "Numerical analysis of the transient behavior of the non-equilibrium quantum liouville equation," *IEEE Trans Nanotechnol*, vol. 17, no. 6, pp. 1197–1205, 2018.

[10] R. K. et al., "A revised wigner function approach for stationary quantum transport," in *Proc. of LSSC*, Springer, 2019, pp. 403–410.

[11] R. V. et al., "Simulating quantum transport in nanoscale transistors: Real versus mode-space approaches," *J. Appl. Phys.*, vol. 92, no. 7, pp. 3730–3739, 2002.

[12] Z. R. et al., "Nanomos 2.5: A two-dimensional simulator for quantum transport in double-gate mosfets," *IEEE Trans. Electron Devices*, vol. 50, no. 9, pp. 1914–1925, 2003.

[13] R. Rosati and F. Rossi, "Scattering nonlocality in quantum charge transport: Application to semiconductor nanostructures," *Phys. Rev. B*, vol. 89, p. 205 415, 20 May 2014. DOI: 10.1103/PhysRevB.89.205415.

[14] W. R. Frensley, "Wigner-function model of a resonant-tunneling semiconductor device," *Phys. Rev. B*, vol. 36, no. 3, p. 1570, 1987.

[15] L. Schulz and D. Schulz, "Formulation of a phase space exponential operator for the wigner transport equation accounting for the spatial variation of the effective mass," *J Comput. Electron*, 2020.

[16] B. A. Biegel and J. D. Plummer, "Comparison of self-consistency iteration options for the wigner function method of quantum device simulation," *Phys. Rev. B*, vol. 54, pp. 8070–8082, 11 Sep. 1996. DOI: 10.1103/PhysRevB.54.8070.